The two-cavity method for characterizing acoustical materials—an interlaboratory study

Martha C Brown[1]
NASA Langley Research Center
Mail Stop 164D, Hampton, VA 23681
[1]martha.c.brown@nasa.gov

Anthony Ciletti[2]
Wichita State University
1845 Fairmont St, Wichita, KS 67260
[2]avciletti@shockers.wichita.edu

Janith Godakawela[3]
Bhisham Sharma[4]
Michigan Technological University
1400 Townsend Dr, Houghton, MI 49931
[3]pgodakaw@mtu.edu
[4]bnsharma@mtu.edu

ABSTRACT

This study focuses on understanding the sound absorption characteristics of porous acoustic materials, which are determined by two key parameters independent of material thickness: characteristic impedance and propagation constant. These parameters can be characterized by testing a porous sample concept in a normal incidence impedance tube using either the two-thickness or the two-cavity method. In the two-thickness method, two samples of varying thicknesses are required. In contrast, the two-cavity method requires testing one sample at two different air cavity depths behind the porous material. This method is particularly advantageous for materials that are costly or challenging to fabricate. This interlaboratory study evaluates the variability of characteristic properties determined using the two-cavity method. Porous acoustic materials were additively manufactured and tested in the Liner Technology Facility (LTF) at NASA Langley Research Center and the Mechanics, Acoustics and Dynamics Lab (MADLab) at Michigan Technological University. The characteristic properties derived from various cavity depth combinations were used to predict the surface impedance of the sample with a rigid backing. The prediction was then compared the measured impedance spectrum. It was also found that the combinations of cavity depths can significantly influence the accuracy of the deduced properties.

1. INTRODUCTION

The acoustic properties of porous bulk absorption materials for no-flow are traditionally characterized using the normal incidence impedance tube testing method. This approach allows for the direct measurement of sound absorption and surface impedance values through two-microphone impedance tube setups. However, accurately determining thickness-independent parameters, such as characteristic impedance and propagation constant, requires the use of more intricate eduction methods such as the two-thickness [1, 2] or two-cavity [3] method. Both methods assume the sample is isotropic, and the characteristic parameters derived are representative of the larger set of samples with similar characteristics. Between these two methods, the two-thickness method requires the impedance tube measurements of two separate samples, where one sample is typically twice the thickness of the other sample to simplify the equations in the model. These surface impedances are used to educe the required characterization parameters. In contrast, the two-cavity method allows the eduction of these parameters using measurements obtained using a single sample that is tested using two different air cavity depths.

This reliance on a single test article is particularly useful in situations where it may be difficult to procure two different sample thicknesses, either due to manufacturability or cost constraints.

This study explores the utility of using the two-cavity method for characterizing the thickness-independent acoustic properties of additively manufactured porous materials. Recent advances in additive techniques have enabled the fabrication of porous materials with complex cellular architectures that were previously infeasible [4]. However, the fabrication of such samples is still relatively expensive, especially those manufactured using metal or ceramic additive methods. Sourcing these materials makes it prohibitively costly to fabricate samples with multiple thicknesses, as necessary for the two-thickness eduction method. Characterizing these materials is further complicated by the replicability issues inherent to different additive manufacturing techniques. These challenges arise from various problems such as thermal expansion in resin-based printing [5], staircasing in extrusion-based printing [6], and keyhole porosities in sintering-based printing [7], all of which hinder the production of samples with the same microstructural features but differing thicknesses.

The overall objective of this interlaboratory collaboration between the Liner Technology Facility at NASA Langley Research Center (LTF) and the Mechanics, Acoustics, and Dynamics Lab (MADLab) at Michigan Technological University is to characterize the uncertainties and biases inherent within the fabrication and acoustic testing of additively manufactured porous materials of interest for aircraft noise reduction applications. To this end, this paper presents the preliminary results comparing acoustic parameters educed using the two-cavity method from porous test samples fabricated using the additive manufacturing facilities at the individual labs. This study specifically focuses on characterizing porous absorbers with triply periodic minimal surface (TPMS) pore geometries [8]. Recent studies have demonstrated that such geometries offer substantial multifunctional performance advantages, including the ability to be customized for broadband noise reduction [9, 10]. In this study, porous samples with the Diamond-based TPMS pore architectures are independently fabricated by both labs using a resin-based additive technique and tested using their individual two-microphone impedance tube test rigs [11, 12]. The measured impedances are then compared and analyzed to gain insights into the effect of manufacturing and testing uncertainties on the measured and predicted acoustic properties.

2. SAMPLE FABRICATION AND MEASUREMENT

Diamond-based TPMS porous structures with strut-based geometries can be generated by finding the isosurface ($U_D = 0$) of the following equation [8]:

$$U_D(\mathrm{x,y,z}) = \sin\left(\frac{2\pi}{a}x\right)\sin\left(\frac{2\pi}{a}y\right)\sin\left(\frac{2\pi}{a}z\right) + \sin\left(\frac{2\pi}{a}x\right)\cos\left(\frac{2\pi}{a}y\right)\cos\left(\frac{2\pi}{a}z\right) + \cos\left(\frac{2\pi}{a}x\right)\sin\left(\frac{2\pi}{a}y\right)\cos\left(\frac{2\pi}{a}z\right) + \cos\left(\frac{2\pi}{a}x\right)\cos\left(\frac{2\pi}{a}y\right)\sin\left(\frac{2\pi}{a}z\right) - t, \quad (1)$$

where *x*, *y*, and *z* are the cartesian coordinates and *a* and *t* control the periodic unit cell length and the volume fraction of the resulting structure, respectively. The strut-based or network-type Diamond structures contain two regions of equal volume separated by the isosurface (Figure 1a). One of these two regions is considered solid and the other void to obtain strut-based Diamond structures (Figure 1b). The overall porosity of the structure is varied by altering the parameter *t*. An implicit field-based modeling method implemented within the software nTopology is used to design samples with 40% and 60% porosities having uniform 3 mm cubic unit cell size. For each porosity, samples are printed at two thicknesses of 25.4 mm and 50.8 mm.

1a. Diamond isosurface 1b. Strut-based Diamond

Figure 1: *Representative unit cells for Diamond TPMS structure.*

The samples were additively manufactured using the VAT photopolymerization stereolithography (SLA) technique. It is a widely used additive manufacturing technique well-suited for printing TPMS samples. SLA printers work by curing a photopolymer resin with a controllable laser. Relative to other additive methods, SLA printers can produce high-resolution prints with fine feature detail and smooth surface finish. These are required qualities for TPMS samples with the desired geometric properties. At LTF, the samples were fabricated using the Accura 60 resin and printed using a 25 µm layer height. At MADLab, a Formlabs Form 3+ resin-based SLA printer setup was used for fabrication. Samples were printed with a layer height of 25 µm using Formlabs' proprietary clear V4 resin. For both sets of samples, the as-printed porosities were estimated based on a weight-based method using the equation:

$$\rho_{fabricated} = \frac{W_{fabricated}}{V_{fabricated} \times \rho_{resin}}, \tag{2}$$

where $W_{fabricated}$ is the measured mass of the sample, $V_{fabricated}$ is the volume of the sample calculated based on sample dimensions, and ρ_{resin} is the density of cured resin, measured by calculating the average density of two 30-mm diameter solid cylinders for both 12.7-mm and 25.4-mm thickness samples.

The fabricated samples were tested under no-flow conditions using the impedance tube test rigs at LTF and MADLab. At LTF, the impedance measurements were performed using a 50.8 mm square cross-section waveguide with a controlled-amplitude, swept-sine noise source, where the input sound was swept through the frequency range from 500 to 3000 Hz. The samples were tested at 120 dB and 140 dB sound pressure levels to analyze the linearity of the samples with respect to incident sound pressure level. At MADLab, the impedance tube tests were conducted using a 38.1 mm square impedance tube manufactured by Mecanum Inc. All tests at MADLab were performed using a white noise signal with a frequency range of 500 to 3000 Hz at an incident sound pressure level of 100 dB.

3. TWO-CAVITY CHARACTERIZATION METHOD

The two-cavity method is used to characterize a uniform porous sample using only one sample, as prescribed by Utsuno et al. [3]. The method is schematically represented in Figure 2, where the incident plane wave is assumed to be traveling from left to right within the impedance tube setup. The reflected plane wave is assumed to be traveling from right to left, which sets up a standing wave pattern in the waveguide. The incident and reflected waves from the impedance discontinuity between the porous material/airspace and the airspace/backplate are not represented to maintain clarity of the image. As per the method, the surface impedance of the uniform porous material of thickness d, ζ_S, is first measured with an air cavity backing depth of L. Then, the cavity depth is changed to L', and the new surface impedance, ζ_S', is measured. The two measurements can then be used to educe the sample's characteristic impedance, ζ_C, and propagation constant, Γ, using Equations 3 and 4, where ζ_1 , ζ_1' are the surface impedances of the air cavity depths L and L', respectively, and calculated using Equations 5 and 6:

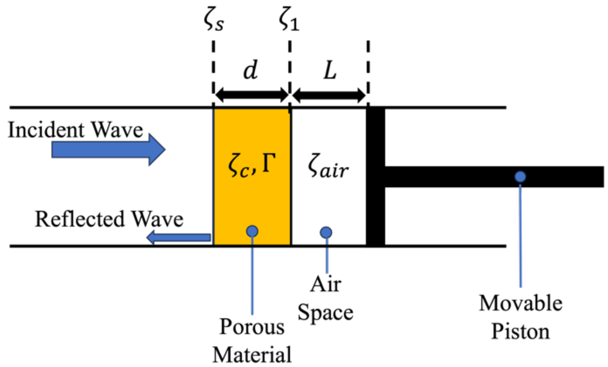

Figure 2: *Schematic diagram representation of the two-cavity characteristic impedance and propagation constant eduction method.*

$$\zeta_C = \sqrt{\frac{\zeta_S\zeta_S'(\zeta_1 - \zeta_1') - \zeta_1\zeta_1'(\zeta_S - \zeta_S')}{(\zeta_1 - \zeta_1') - (\zeta_s - \zeta_S')}} \tag{3}$$

$$\Gamma = \frac{1}{2jd} ln\left[\frac{(\zeta_S + \zeta_C)(\zeta_1 - \zeta_C)}{(\zeta_S - \zeta_C)(\zeta_1 + \zeta_C)}\right] \tag{4}$$

$$\zeta_1 = -j\zeta_{air} cot\ (kL) \tag{5}$$

$$\zeta_1{}' = -j\zeta_{air} cot\ (kL'). \tag{6}$$

It is notable that all the above values are complex numbers, requiring the unwrapping of the phase constant, which is the imaginary part of Γ. Further, while the cavity depths may be chosen arbitrarily, one must be careful about the possible elimination of terms at specific frequencies, depending on the speed of sound in the saturating medium and the difference in the cavity depths. In this investigation, cavity depths were chosen such that this condition does not begin to occur until frequencies are higher than the test range. Specifically, in this study, the authors explored a two-cavity depth combination of 25.4 mm and 50.8 mm.

4. RESULTS

Acoustic tests were conducted in the LTF normal incidence impedance tube at 120 and 140 dB to confirm that the samples were linear, meaning that the acoustic response is independent of sound pressure level. Results showed that all the samples tested were linear. For this reason, the results presented herein will be limited to those for data acquired with a source level of 120 dB. Figure 3 shows a comparison of measured normalized surface impedance results between LTF and MADLab for a 50.8 mm depth sample. The impedance results were normalized to the characteristic impedance of air. Resonance occurs at the frequency where the reactance crosses the zero axis with a positive slope. Antiresonance occurs at the frequency where the reactance crosses the zero axis with a negative slope. For the 40% porosity case (Figure 3a), the frequency of peak resistance for the MADLab sample is lower than for the LTF sample. For the 60% porosity case (Figure 3b), the frequency of peak resistance was lower than for the LTF sample. This trend was experienced in all the samples. Slight differences in porosities could be a contributing factor. It is evident that differences between as-designed and as-printed samples can impact results. The significant difference in results shows that additional tuning to the SLA process is required to ensure a better match between the two laboratories. Next, the authors implemented the two-cavity method to their respective datasets to determine the effectiveness of this characterization method.

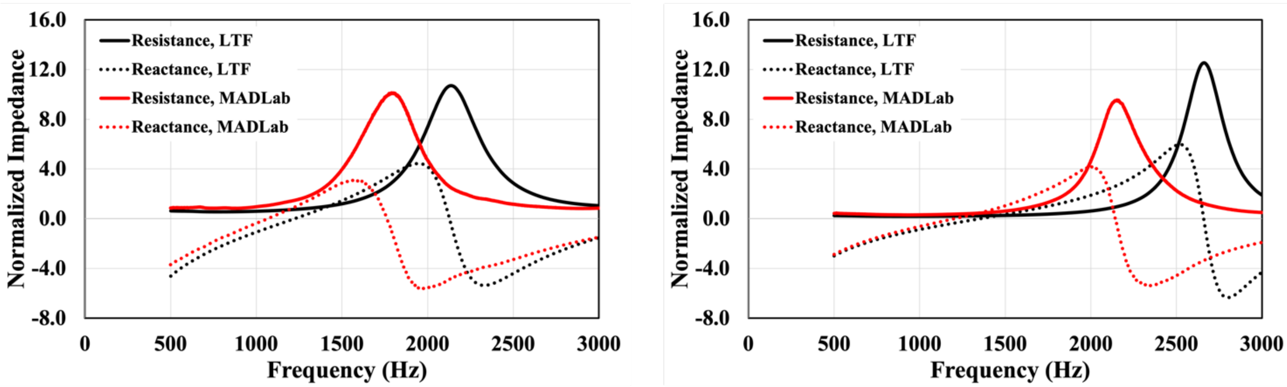

a: 40% porosity. b: 60% porosity.

Figure 3: *Comparison of measured LTF and MADLab normalized impedance spectra, 50.8 mm-depth sample.*

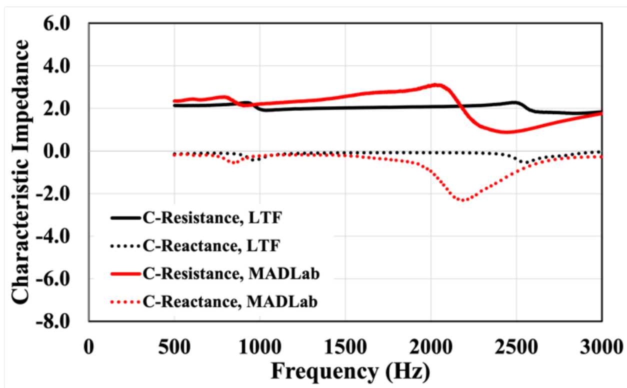

Figure 4: *Comparison of normalized characteristic impedances from LTF and MADLab, 60% porosity, 50.8 mm-depth sample; cavity combination: 25.4 mm, 50.8 mm.*

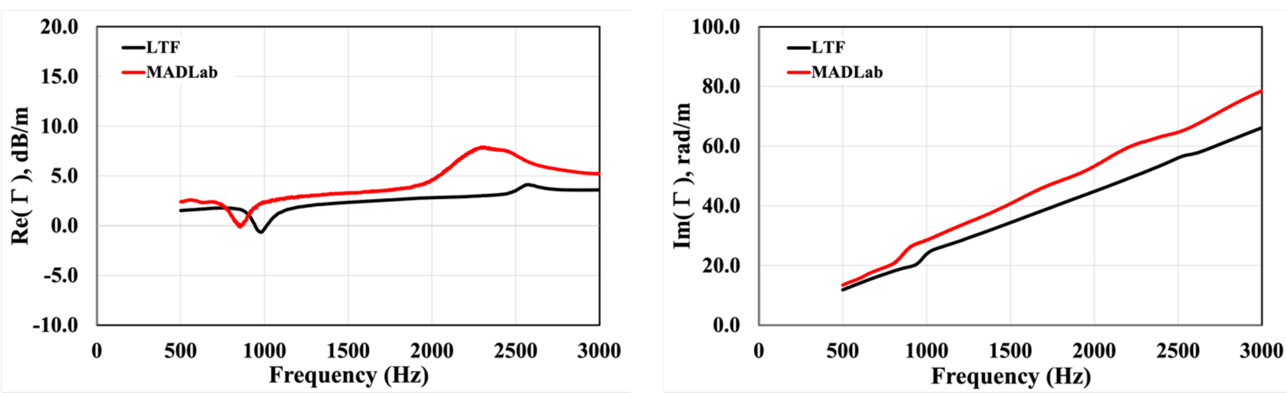

a: Real Component, Γ. b: Imaginary Component, Γ.

Figure 5: *Comparison real and imaginary components of propagation constant from LTF and MADLab, 60% porosity, 50.8 mm-depth sample; cavity combination: 25.4 mm, 50.8 mm.*

A porous sample is characterized by its characteristic impedance and propagation constant. These intrinsic parameters were compared for samples constructed at both facilities to determine if there were any disparities in the data. Figures 4 and 5 show the characteristic impedance and propagation constant, respectively, of a 60% porosity, 50.8 mm-depth sample. In Figure 4, LTF results show a disparity around 2500 Hz, and MADLab results show a disparity around 2000 Hz. In Figure 5a, the real component of the propagation constant shows that the results are continuous between 1000 and 2000 Hz. There are a number of potential reasons for this. In Figure 5b, the imaginary component of the propagation constant shows that this sample from MADLab has a higher phase shift than LTF over the measured frequency range. These reasons include, but are not limited to, phase unwrapping not applied properly, cavity depth combinations that may not be ideal, or printed samples may be nonuniform. Further examination is needed in these areas to improve the comparison of results.

Taking each laboratory's respective intrinsic parameters, the predicted surface impedance for the same sample but with a rigid (i.e., zero cavity) backing was computed and compared with measured results. Figure 6 compares the measured and predicted results for a 50.8 mm-depth sample. In Figure 6a, the LTF results compare well up to 2500 Hz, and the MADLab results (Figure 6b) compare better than the LTF results over the measured frequency range. These preliminary results show that more work is needed to better utilize the two-cavity method for characterizing TPMS structures.

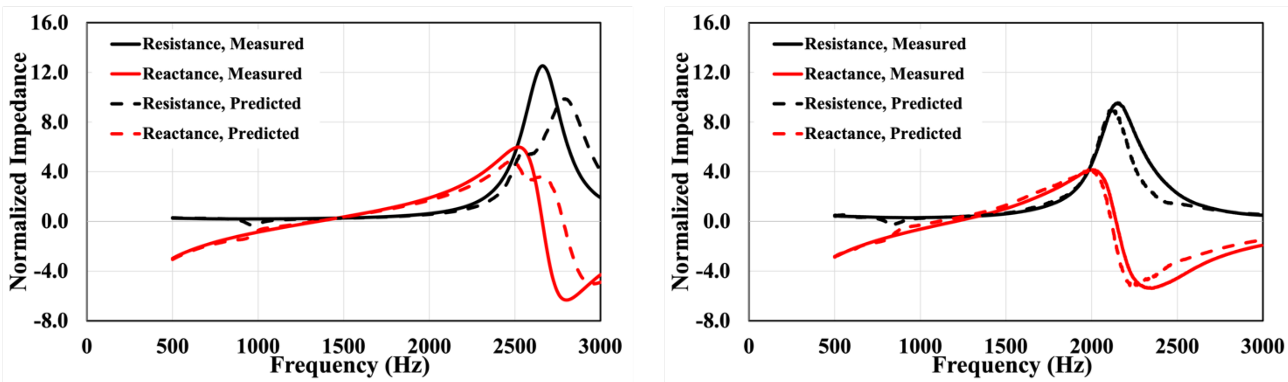

a: Measured vs. Predicted, LTF. b: Measured vs. Predicted, MADLab.

Figure 6: *Comparison of measured vs. predicted impedance spectra from each facility, 60% porosity, 50.8 mm-depth sample, cavity combination: 25.4 mm, 50.8 mm.*

5. CONCLUSIONS

The objective of this interlaboratory collaboration was to characterize the uncertainties and biases within the fabrication and acoustic testing of additively manufactured porous materials. The two-cavity method was used in characterizing the acoustic properties of additively manufactured porous materials. The Diamond TPMS structure at 40% and 60% porosity was shown to be linear. The differences in measured results between the Liner Technology Facility and MADLab demonstrate the need to better understand the effects of differences between as-designed and as-built samples on the resultant impedance achieved with this type of liner design. Preliminary results also showed that more analysis is needed to properly use the two-cavity method for this type of material, including the selection of the two cavity depth combinations.

ACKNOWLEDGMENTS

The authors would like to thank Alonzo (Max) Reid and Scott Angler for NASA testing and Robert Andrews for stereolithography services. This work was funded by the Advanced Air Transport Technology Project of the Advanced Air Vehicles Program.

REFERENCES

[1] D.L. Palumbo, M.G. Jones, J. Klos, J. Park, Improvements to the two-thickness method for deriving acoustic properties of materials, *INTER-NOISE and NOISE-CON Congress and Conference Proceedings, Institute of Noise Control Engineering, (2004).*

[2] M.G. Jones, W.R. Watson, B.M. Howerton, S. Busse-Gerstengarbe, Comparative study of impedance eduction methods, Part 2: NASA tests and methodology, *19th AIAA/CEAS Aeroacoustics Conference*, (*2013*), p. 2125.

[3] H. Utsuno, T. Tanaka, T. Fujikawa, A.F. Seybert, Transfer-Function Method for Measuring Characteristic Impedance and Propagation Constant of Porous Materials, *Journal of the Acoustical Society of America* ***86****(2) (1989)* 637-643.
[4] S. Guddati, A.S.K. Kiran, M. Leavy, S. Ramakrishna, Recent advancements in additive manufacturing technologies for porous material applications, *International Journal of Advanced Manufacturing Technology* ***105****(1-4) (2019)* 193-215.
[5] A. Lomte, B. Wojciechowski, B. Sharma, A comparison of the two and four microphone methods for deriving the characteristic acoustic properties of porous materials, *INTER-NOISE and NOISE-CON Congress and Conference Proceedings, Institute of Noise Control Engineering, (2020)*, pp. 4111-4122.
[6] B. Wojciechowski, Y.T. Xue, A. Rabbani, J.S. Bolton, B. Sharma, Additively manufactured spinodoid sound absorbers, *Additive Manufacturing* ***71*** *(2023)* 103608.
[7] A. Sola, A. Nouri, Microstructural porosity in additive manufacturing: The formation and detection of pores in metal parts fabricated by powder bed fusion, *Journal of Advanced Manufacturing and Processing* ***1****(3) (2019)* e10021.
[8] A.H. Schoen, Infinite periodic minimal surfaces without self-intersections, National Aeronautics and Space Administration (1970).
[9] J.W. Feng, J.Z. Fu, X.H. Yao, Y. He, Triply periodic minimal surface (TPMS) porous structures: from multi-scale design, precise additive manufacturing to multidisciplinary applications, *International Journal of Extreme Manufacturing* ***4****(2) (2022)* 022001.
[10] B. Wojciechowski, K. Wetter, C. Cheepa, B. Sharma, Acoustic properties of 3D printed bulk absorbers with novel surface topologies, *INTER-NOISE and NOISE-CON Congress and Conference Proceedings, Institute of Noise Control Engineering, (2019)*, pp. 565-572.
[11] J. Y. Chung and D. A. Blaser, "Transfer function method of measuring in-duct acoustic properties. I. Theory," *Journal of the Acoustical Society of America*, ***68*** *(1980)* 907–913.
[12] M.G. Jones, W.R. Watson, D.M. Nark, B.M. Howerton, & M.C. Brown, (2020, April). A Review of Acoustic Liner Experimental Characterization at NASA Langley, NASA-TP-220583.